

17th CIRP Conference on Modelling of Machining Operations

Comparison of bone temperature elevation in drilling of human, bovine and porcine bone

Mohd Faizal Ali Akhbar^a and Ahmad Razlan Yusoff^{b*}

^a Faculty of Engineering Technology, Universiti Malaysia Pahang, 26300 Kuantan, Pahang, Malaysia

^b Faculty of Manufacturing Engineering, Universiti Malaysia Pahang, 26600 Pekan, Pahang, Malaysia

* Corresponding author. Tel.: +60139339934. E-mail address: razlan@ump.edu.my

Abstract

This paper compares the maximum temperature elevation in human, bovine and porcine bone corresponding to the drilling rotational speed from 1,000 to 10,000 rev/min. For this purpose, we perform drilling simulation using human, bovine and porcine bone models combined with experimental validation process. We demonstrate numerically and experimentally that bovine bone can mimic the human bone in terms of temperature elevation in bone drilling (0.49 – 1.15% error). The increasing rotational speed gives rise to the maximum bone temperature. The results indicate that the drilling simulation can be used to approximate the reasonably accurate output in biomedical research.

© 2019 The Authors. Published by Elsevier B.V.

Peer-review under responsibility of the scientific committee of The 17th CIRP Conference on Modelling of Machining Operations

Keywords: bone drilling; finite element; temperature elevation; bovine; porcine; human

1. Introduction

The investigation in bone-drilling research requires access to precise and dependable substitute bone model for human bone to enable progressions in the area. This is because of the difficulty of obtaining human bone for experimental purposes. Moreover, there are ethical limitations related with the procurement and usage of human bone [1].

Artificial [2] and animal bone models such as bovine [1,3,4] and porcine [5–7] have been used extensively by researchers in bone-drilling studies as the substitute for human bone. The artificial bone is expensive and their reliability is debatable [1]. Animal bone has shown a high reliability, abundantly available and cheap [1,3,8,9]. Fletcher et al. [1] unveiled that young bovine bone has a similar macroscopic dimension to adult human bone and biomechanically resembles human long bone. Furthermore, bovine bone provides a better availability, uncomplicated storage and a cheaper alternative compared with artificial and

human bones. Augustin et al. [5] tested their newly developed step drill bit on porcine femur to investigate bone temperature rise during the drilling process and concluded that the porcine bone is the best substitute for human bone. However, authors offer no explanation to justify their claim.

Numerous researchers have claimed that both bovine and porcine specimens closely mimic human bone in terms of structure and thermal behavior. However, to the best of author's knowledge, there is no study compares the thermal performance among human, bovine and porcine bone during the bone-drilling process to validate this claim. Therefore, in this work, we simulate the bone-drilling process with three different bone models (human, bovine and porcine) to evaluate the maximum bone temperature trend corresponding with the rotational speed of 1,000 to 10,000 rev/min. Then, we validate the simulation results with experimental bone drilling test. The resulting outcomes from this study can be capitalized as the guidelines to choose appropriate substitute for human bone in bone-drilling research. If the drilling

simulations are shown to be valid, this will offer a considerable change to the typical bone drilling practice as it offers a cost-effective and feasible alternative to the more expensive experimental methods used currently.

2. Materials and methods

2.1. FEM drilling simulation setup

In this study, the drill bit and bone model (Fig. 1) were constructed with the DEFORM-3D software in the pre-simulation process.

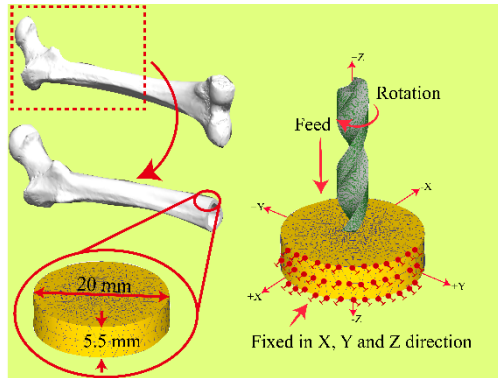


Fig. 1. FEM drilling setup.

The thermal and mechanical properties of human, bovine and porcine bone in Table 1 was manually inserted in the finite element software for workpieces setup.

Table 1. Thermal and mechanical properties for human, bovine and porcine cortical bone [8,10–13].

Properties	Human	Bovine	Porcine
Density (kg m^{-3})	2100	2000	1640
Young's modulus (GPa)	17	22	16.7
Poisson's ratio	0.4	0.33	0.3
Specific heat ($\text{J kg}^{-1} \text{K}^{-1}$)	1260	1300	1640
Thermal conductivity ($\text{W m}^{-1} \text{K}^{-1}$)	0.38	0.3	0.45

To set up the correct bone models, a correct material model is required. We adopted the flow stress equation in Eq. (1) to estimate the stress-strain curve in the bone models.

$$\sigma(\varepsilon_p, \dot{\varepsilon}_p, T) = c \cdot \varepsilon_p^n \cdot \dot{\varepsilon}_p^m \cdot \left(\frac{T}{T_0}\right)^{-r} + y \quad (1)$$

Where ε_p is plastic strain, $\dot{\varepsilon}_p$ is plastic strain rate, T is temperature, T_0 is the room temperature and c , n , m , r and y are the coefficients, which were obtained through curve fitting process (Fig. 2) [6] with the experimental data from Melnis and Knets [14]. The damage criterion of Cockroft and Latham (Eq. (2)) was used for the chip separation because mechanic fracture in cortical bone is comparable with the ductile damage as reported in [15].

$$D = \int_0^{\varepsilon_{eff}} \left(\frac{\sigma_{max}}{\sigma_{eff}} \right) d\varepsilon \quad (2)$$

Where D is the critical damage value, ε_{eff} is the effective fracture strain, $d\varepsilon$ is the effective stress and σ_{max} is the maximum stress. When the damage value exceeds the critical damage, the bone elements will be deleted [15]. The initial temperature of the drill bit and bone models were assumed to be 30 °C and 37 °C, respectively. The shear friction factor of 0.3 was obtained from the previous literature [16] and was adopted for the tool-workpiece interface.

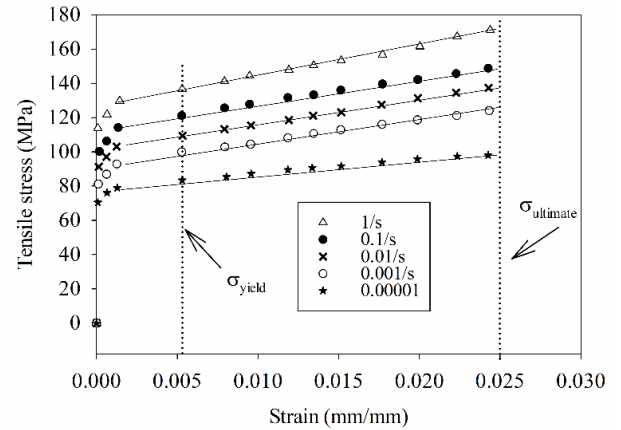


Fig. 2. Stress-strain curve from Melnis and Knets [14].

The incremental Lagrangian mesh was used for the material deformation because it enables the drilling simulation to restart the at the point where it was stopped due to crash or error. In this study, the drill bit was set as a rigid object while bones were modeled as plastic objects, which mean that they can be simply deformed and cut by the drill bit. When the mesh distorts, it will be automatically remeshed before further cutting process. The finer mesh was set to be generated at the center of bone model and coarser mesh was applied at the other area for minimum computational time. The size ratio between the coarser and finer mesh was set at 1:7. The minimum mesh size for bone model was 0.36 mm. The drill bit was meshed with approximately 20,000 elements with the size ratio of 10, which was recommended by the manufacturer [17]. The movement of the bone model was restricted; the speed in the X, Y and Z axes is set to 0 (Fig. 1).

Drilling parameters and drill bit geometry such as feed rate = 0.13 mm/rev, hole depth = 5 mm, drill bit diameter = 4.5 mm, point angle = 118° and helix angle = 30° were kept constant throughout the drilling process.

3. Results and discussion

3.1. Maximum bone temperature

Fig. 3 displays the maximum bone temperatures obtained at various rotational speeds (1,000 rev/min to 10,000 rev/min)

from three different bone models (human, bovine, and porcine). All the bone models showed a positive linear relationship in terms of maximum bone temperature and rotational speed. Human bone temperature elevations were in the range of 49.2 to 64.3 °C and bovine bone displayed a similarity in terms of elevations range (48.9 - 63.5 °C). Increasing rotational speed causes increase in the friction energy between the drill bit-bone and bone debris-drilling hole wall. Majority of this energy will be converted into heat and thus, increasing the bone temperature [3,4,7,18–20].

The blue, red and green lines represent the bone temperature trends for human, bovine and porcine bone, respectively. As can be seen from the bone temperature trends (regression lines), bovine bone closely resembles human bone in terms of temperature elevation in bone drilling. The recorded maximum bone temperatures in bovine bone model were varied from 0.49 – 1.15 % compared with the bone temperatures discovered in human bone. This similarity might be due to the close value of the thermal conductivity (0.38 and $0.33 \text{ W m}^{-1} \text{ K}^{-1}$) and specific heat (1260 and $1300 \text{ J kg}^{-1} \text{ K}^{-1}$) between both species. Different bones absorb heat at different rates due to the various structural and thermal properties' factors. With the low thermal conductivity of both bone types, the cumulated heat is unable to be dissipated easily, thus increasing the bone temperature. The bone's specific heat is defined as the energy required to increase the temperature of 1 kg of bone by 1 °C; the amount of heat required for elevation in bovine and human bone approximately similar.

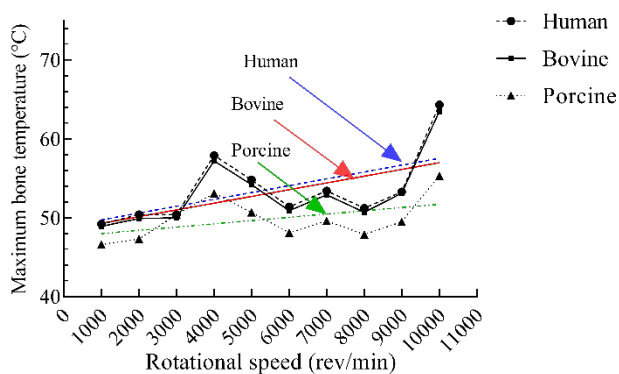


Fig. 3. Maximum bone temperature corresponding with rotational speed in drilling simulation.

The mechanical properties of bones also contribute to the temperature rise in bone drilling. Bovine bone's density has been tipped to be suitable for human bone substitute for use in orthopedic research [1]. The normal range of healthy human bone density is from 1.057 to 1.223 g cm^{-3} [21] and very closely match the density of bovine bone in [1] ranging from 1.93 to 1.98 g cm^{-3} . Due to this close similarity in bone density, the cutting forces required to cut both bone types are approximately similar. Thus, the bone temperatures display similar trend and close elevation ranges. Furthermore, bovine bone mechanical properties also reliable and consistence, which presents the important aspect required as the substitute

for human bone to facilitate the related biomedical research [1,8]. Also, the cost of bovine bone is minimal compared to artificial or cadaveric human bone and can be obtained easily as part of the food chain in anywhere. The ethical constrain regarding the utilization of bovine bone also nominal.

Our bone models only focus on cortical bone drilling and exclude the effect of trabecular bone. This is to simplify the bone model and minimize the computation time for the drilling process. However, the effect is negligible because in the real bone drilling process, the maximum bone temperatures were discovered when drilling the cortical bone due to their compactness and high density [22]. Since our objective was to investigate the maximum bone temperature, the inclusion of trabecular bone is assumed irrelevant.

3.2. Validation of bone model with bone drilling experiment

To validate the simulation results, we performed ex-vivo bone drilling test under laboratory-controlled condition and the drilling setup is shown in Fig. 4. Bone specimens were collected from the local butcher after four hours of slaughter. No animal was harmed for the purposed of this test. The mid diaphysis of bovine femur was excised using hack saw ($130.78 \pm 0.01 \text{ mm}$). Soft outer tissue (periosteum) was removed from the bone to avoid the clogging of the drill bit's flute. Surface of the cortical bone was milled to facilitate for a smooth entry of drill bit and accurate drilling hole depth as the depth was measured from the top flat surface. Bone drilling test was performed with conventional milling machine GATE PBM 2000 (the United Kingdom) using 4.5 mm diameter carbide drill bit with point angle of 118° and helix angle of 30° . The temperature measurement was recorded with data logger OMRON ZR-RX25 (Japan) with K-type thermocouple. Four thermocouple holes (1 mm diameter) was created 0.5 mm from the drilling hole at the depth of 3 mm. The average of maximum bone temperatures was calculated for the validation of bone model. Thermal paste was used to fill the thermocouples holes to eliminate the effect of air gap in the drilling hole. The drilling test was performed at constant feed rate of 0.13 mm/rev and hole depth of 5 mm. Maximum bone temperatures corresponding with rotational speed of 1,000, 2,000 and 3,000 rev/min were recorded and compared with FEM results.

The results from the drilling simulation and experimental bone drilling test are shown in Fig. 5. Both of the simulation and experimental methods depicted a directly proportional relationship between rotational speed and bone temperature elevation. The temperature elevation differences were in the range of 1.3 to $2.7 \text{ }^\circ\text{C}$. The bone temperature in drilling simulations were 42.0 , 42.5 and $42.7 \text{ }^\circ\text{C}$ for rotational speed of 1000, 2000 and 3000 rev/min, respectively. By using Lee et al. [23] bone temperature approximation method, the 1000, 2000 and 3000 rev/min rotational speed produced bone temperatures of 39.3 , 40.0 and $41.3 \text{ }^\circ\text{C}$, respectively. The errors between drilling simulation and experimental bone drilling were in the range of 3.2 to 6.8% . Therefore, it can be

said that our FEM results are reasonably accurate for bone drilling temperature approximation.

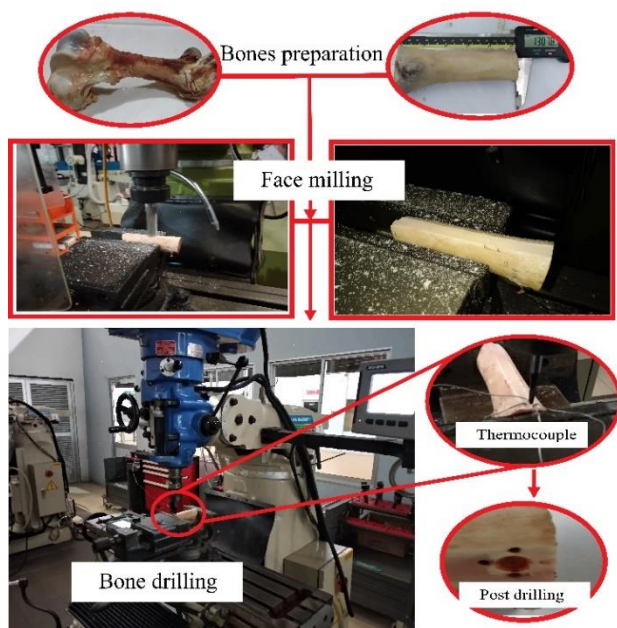


Fig. 4. Experimental bone drilling using bovine femurs.

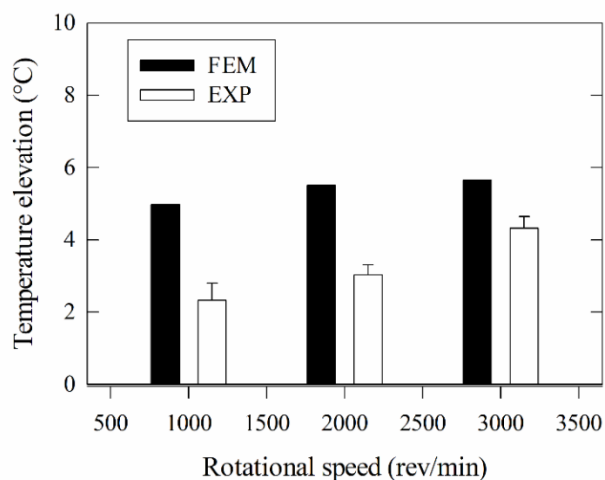


Fig. 5. Comparison of results from FEM and experimental (EXP) bone drilling.

4. Conclusions

This study was carried out to compare the temperature elevation in human, bovine and porcine bones using drilling simulation and evaluate the appropriate bone model to substitute human bone as the specimens in the biomedical research. From this work, it can be deduced that:

1. Bovine bone closely resembles human bone in terms of maximum bone temperature rise during bone drilling process compared with porcine bone.

2. The maximum bone temperatures correlate positively with rotational speed regardless of bone model types.

3. FEM simulation can approximate the temperature rise in bone drilling accurately.

Whilst obtaining the human bone is difficult, this research will serve as a basis for future studies in biomedical research to enhance our understanding in choosing the suitable substitute for human bone.

Acknowledgements

The authors of this paper would like to thank the Universiti Malaysia Pahang (UMP) for funding this research project under the research grant RDU 170372 and RDU 190124.

References

- [1] J.W.A. Fletcher, S. Williams, M.R. Whitehouse, H.S. Gill, E. Preatoni, *Sci. Rep.* 8 (2018) 10181.
- [2] M.G. Fernandes, E.M.M. Fonseca, R.J. Natal, *J. Brazilian Soc. Mech. Sci. Eng.* 38 (2016) 1855–1863.
- [3] M.F.A. Akhbar, A.R. Yusoff, *Technol. Heal. Care* 1 (2018) 1–15.
- [4] J. Sui, N. Sugita, M. Mitsuishi, *J. Manuf. Sci. Eng.* 137 (2015) 061008.
- [5] G. Augustin, S. Davila, T. Udiljak, T. Staroveski, D. Brezak, S. Babic, *Int. Orthop.* 36 (2012) 1449–1456.
- [6] L. Qi, X. Wang, M.Q. Meng, *Int. j. Numer. Method. Biomed. Eng.* 30 (2014) 845–856.
- [7] G. Augustin, S. Davila, K. Mihoci, T. Udiljak, D.S. Vedrinar, A. Antabak, *Arch. Orthop. Trauma Surg.* 128 (2007) 71–77.
- [8] G. Singh, V. Jain, D. Gupta, A. Ghai, *J. Mech. Behav. Biomed. Mater.* 62 (2016) 355–365.
- [9] M.F. Ali Akhbar, A.R. Yusoff, *Proc. Inst. Mech. Eng. Part H J. Eng. Med.* 233 (2019) 207–218.
- [10] R. Huiskes, *Acta Orthop. Scand.* 185 (1979) 62–63.
- [11] Y.-K. Tu, L.-W.W. Chen, J.-S.S. Ciou, C.-K.K. Hsiao, Y.C. Chen, *J. Med. Biol. Eng.* 33 (2013) 269.
- [12] a M. O'Mahony, J.L. Williams, P. Spencer, *Clin. Oral Implants Res.* 12 (2001) 648–57.
- [13] S.S. Kohles, *J. Mater. Sci. Mater. Med.* 11 (2000) 261–265.
- [14] Melnis, *Knets, Mech Compos Mater* 18 (1982) 358–63.
- [15] R.K. Nalla, J.H. Kinney, R.O. Ritchie, *Nat. Mater.* 2 (2003) 164–168.
- [16] A. Mellal, H.W.A. Wiskott, J. Botsis, S.S. Scherrer, U.C. Belser, *Clin. Oral Implants Res.* 15 (2004) 239–248.
- [17] DEFORM 3D Version 11.0, User's Manual, Version 11, Scientific Forming Technologies Corporation, 2545 Farmers Drive, Suite 200 Columbus, Ohio., 2014.
- [18] M.F.A. Akhbar, M. Malik, A.R. Yusoff, in: *AIP Conf. Proc.*, 2018, p. 020002.
- [19] N.A. Omar, J.C. McKinley, *Foot* 35 (2018) 63–69.
- [20] M. Aghvami, J.B. Brunski, U. Serdar Tulu, C. Chen, J.A. Helms, *J. Biomech. Eng.* 140 (2018) 101010.
- [21] S. Maillane-Vanegas, R.R. Agostinete, K. R. Lynch, I. H. Ito, R. Luiz-de-Marco, M.A. Rodrigues-Junior, B.C. Turi-Lynch, R. A. Fernandes, *J. Clin. Densitom.* (2018).
- [22] J. Lee, C.L. Chavez, J. Park, *J. Biomech.* 71 (2018) 4–21.
- [23] J. Lee, O.B. Ozdoganlar, Y. Rabin, *Med. Eng. Phys.* 34 (2012) 1510–1520.